New Phytologist

Desmethyl butenolides are optimal ligands for karrikin receptor proteins

Journal:	*New Phytologist*
Manuscript ID	NPH-MS-2020-35109.R1
Manuscript Type:	MS - Regular Manuscript
Date Submitted by the Author:	15-Jan-2021
Complete List of Authors:	Yao, Jiaren; The University of Western Australia, School of Molecular Sciences; The University of Western Australia, ARC Centre of Excellence in Plant Energy Biology Scaffidi, Adrian; The University of Western Australia, School of Molecular Sciences Meng, Yongjie; The University of Western Australia, School of Molecular Sciences; Sichuan Agricultural University, Department of Plant Physiology and Biotechnology Melville, Kim; The University of Western Australia, School of Molecular Sciences; The University of Western Australia, ARC Centre of Excellence in Plant Energy Biology Komatsu, Aino; Tohoku Daigaku Daigakuin Seimei Kagaku Kenkyuka, Graduate School of Life Sciences Khosla, Aashima; University of California Riverside, Department of Botany and Plant Sciences Nelson, David; University of California Riverside, Department of Botany and Plant Sciences Kyozuka, Junko; Tohoku Daigaku Daigakuin Seimei Kagaku Kenkyuka, Graduate School of Life Sciences Flematti, Gavin; The University of Western Australia, School of Molecular Sciences Waters, Mark; The University of Western Australia, School of Molecular Sciences; The University of Western Australia, ARC Centre of Excellence in Plant Energy Biology
Key Words:	butenolide, karrikin, strigolactone, plant hormone, differential scanning fluorimetry, intrinsic tryptophan fluorescence, α/β-hydrolase

Desmethyl butenolides are optimal ligands for karrikin receptor proteins

Jiaren Yao[1,2], Adrian Scaffidi[1], Yongjie Meng[1,2], Kim T Melville[1,2], Aino Komatsu[3], Aashima Khosla[4], David C Nelson[4], Junko Kyozuka[3], Gavin R Flematti[1], Mark T Waters[1,2]

[1]School of Molecular Sciences and [2]ARC Centre of Excellence in Plant Energy Biology, The University of Western Australia, Perth, 6009, Australia

[3]Graduate School of Life Sciences, Tohoku University, Sendai, 980-8577, Japan

[4]Department of Botany and Plant Sciences, University of California, Riverside, CA, 92521 USA

For correspondence: mark.waters@uwa.edu.au; +61 8 6488 4405

Word count	
Summary	194
Introduction	1308
Materials and Methods	1068
Results	2337
Discussion	1728
Acknowledgements	54
References	2220
TOTAL	**6441 (Intro, M&M, Results & Discussion)**
Number of Figures	5
Number of Tables	0
Supporting Information Files	1

SUMMARY

- Strigolactones and karrikins are butenolide molecules that regulate plant growth. They are perceived via the α/β-hydrolase DWARF14 (D14) and its homologue KARRIKIN INSENSITIVE2 (KAI2), respectively. Plant-derived strigolactones have a butenolide ring with a methyl group that is essential for bioactivity. By contrast, karrikins are abiotic in origin, and the butenolide methyl group is non-essential. KAI2 is probably a receptor for an endogenous butenolide, but the identity of this compound remains unknown.
- Here we characterise the specificity of KAI2 towards differing butenolide ligands using genetic and biochemical approaches.
- We find that KAI2 proteins from multiple species are most sensitive to desmethyl butenolides that lack a methyl group. Desmethyl-GR24 and desmethyl-CN-debranone are active via KAI2 but not D14. They are more potent KAI2 agonists than their methyl-substituted reference compounds both *in vitro* and in plants. The preference of KAI2 for desmethyl butenolides is conserved in *Selaginella moellendorffii* and *Marchantia polymorpha*, suggesting that it is an ancient trait in land plant evolution.
- Our findings provide insight into the mechanistic basis for differential ligand perception by KAI2 and D14, and support the view that the endogenous substrates for KAI2 and D14 have distinct chemical structures and biosynthetic origins.

INTRODUCTION

Butenolides are a class of unsaturated lactones containing a four-carbon heterocyclic ring. A diverse collection of carotenoid-derived butenolides known as strigolactones have wide-ranging hormonal activity in the regulation of shoot and root architecture in plants, and important roles in root-rhizosphere signalling (Al-Babili & Bouwmeester, 2014; Wang *et al.*, 2015; Waters *et al.*, 2017). Another set of butenolides that regulate plant growth are karrikins, which are produced abiotically from burnt vegetation (Flematti *et al.*, 2004). Karrikins promote seed germination and seedling photomorphogenesis. Several species appear to have adapted to fire-prone environments by evolving increased sensitivity to karrikins (Flematti *et al.*, 2007; Nelson *et al.*, 2012; Sun *et al.*, 2020).

Strigolactones and karrikins are recognised through homologous α/β-hydrolase receptor proteins, namely DWARF14/DECREASED APICAL DOMINANCE2 (D14/DAD2) and KARRIKIN INSENSITIVE2/HYPOSENSITIVE TO LIGHT (KAI2/HTL). D14 orthologues are restricted to seed plants, whereas KAI2 orthologues are ubiquitous amongst land plants. KAI2 is likely to be the ancestral α/β-hydrolase from which D14 arose (Delaux *et al.*, 2012; Waters *et al.*, 2012; Bythell-Douglas *et al.*, 2017; Walker *et al.*, 2019). D14 and KAI2 bind and regulate the activity of F-box protein MORE AXILLARY BRANCHES2 (MAX2, orthologous to DWARF3 in rice). MAX2 acts within an SCF-type E3 ubiquitin ligase complex to target members of the SUPPRESSOR-OF-MAX2-1 (SMAX1)-LIKE (SMXL) family for polyubiquitination and proteasomal degradation (Zhao *et al.*, 2015; Yao *et al.*, 2016; Shabek *et al.*, 2018). MAX2 is recruited to specific SMXL protein substrates by D14 and KAI2. Activation of D14 by strigolactones induces degradation of SMXL6, SMXL7 and SMXL8 proteins of Arabidopsis (collectively orthologous to DWARF53 in rice) to bring about the transcriptional and physiological changes that define the strigolactone response (Jiang *et al.*, 2013; Zhou *et al.*, 2013; Soundappan *et al.*, 2015; Wang *et al.*, 2015; Liang *et al.*, 2016; Wang *et al.*, 2020). By contrast, KAI2 promotes the removal of SMAX1 and SMXL2 in Arabidopsis, and of SMAX1 orthologues in rice and *Lotus*, thereby regulating seed germination, seedling photomorphogenesis, root morphology and arbuscular mycorrhizal symbiosis (Stanga *et al.*, 2013; Stanga *et al.*, 2016; Swarbreck *et al.*, 2019; Villaécija-Aguilar *et al.*, 2019; Bunsick *et al.*, 2020; Carbonnel *et al.*, 2020; Choi *et al.*, 2020; Khosla *et al.*, 2020; Wang *et al.*, 2020; Zheng *et al.*, 2020). In some cases, the division of labour

between D14 and KAI2 is not so clear-cut. In rice, mesocotyl elongation is regulated by both D14- and KAI2-dependent processes through OsSMAX1 (Zhao *et al.*, 2015), while in Arabidopsis, exogenous strigolactones trigger degradation of SMXL2 by activating D14, thus establishing a potential mechanism for convergence of SL and KAR signalling (Wang *et al.*, 2020).

D14 and KAI2 proteins are hydrolase enzymes that have activity towards various strigolactone analogues (Hamiaux *et al.*, 2012; Tsuchiya *et al.*, 2015; Waters *et al.*, 2015b; de Saint Germain *et al.*, 2016; Uraguchi *et al.*, 2018; Yao *et al.*, 2018). Based on their biochemical similarities and close homology, KAI2 and D14 recognise similar compounds and likely have similar modes of action. Ligand hydrolysis, mediated by a highly conserved catalytic triad of Ser-Asp-His residues, likely begins with nucleophilic attack by the serine residue upon a suitable carbonyl group, as found on the butenolide moiety (Scaffidi *et al.*, 2012; de Saint Germain *et al.*, 2016; Yao *et al.*, 2016). Mutations in the catalytic serine render both D14 and KAI2 incapable of hydrolysis and signalling (Hamiaux *et al.*, 2012; Waters *et al.*, 2015b), but mutation of the aspartic acid residue in Arabidopsis D14 abolishes hydrolysis while leaving the signalling function intact (Seto *et al.*, 2019). Although ligand hydrolysis appears to be a conserved feature of butenolide signalling, the precise role of ligand hydrolysis in receptor activation remains uncertain (Marzec & Brewer, 2019; Yao & Waters, 2019; Bürger & Chory, 2020b).

Irrespective of how D14 is activated, ligand hydrolysis leads to the formation of a reaction intermediate whereby a derivative of the butenolide ring becomes covalently attached to the catalytic histidine of the receptor (de Saint Germain *et al.*, 2016; Yao *et al.*, 2016; Bürger *et al.*, 2019). In differential scanning fluorimetry (DSF) experiments, both D14 and KAI2 undergo a ligand-induced decrease in melting temperature (T_m) upon exposure to a bioactive ligand, and there is a strong correlation between the bioactivity of a ligand and its propensity to trigger a decrease in T_m (Abe *et al.*, 2014; Yao *et al.*, 2018; Seto *et al.*, 2019). Notably, a structural analysis revealed partial collapse of the lid domain of D14 when complexed with D3 (the rice orthologue of MAX2) in the presence of GR24 (Yao *et al.*, 2016). Accordingly, the decrease in the melting temperature of D14 and KAI2 observed in DSF assays has been widely interpreted to represent the transition of the receptor into an activated state (Seto *et al.*, 2019; Chesterfield *et al.*, 2020).

Although KAI2 is required for plant responses to karrikins, it is hypothesized that KAI2 is a receptor for another intrinsic butenolide that karrikins, or a karrikin metabolite, mimic (Waters *et al.*, 2015b; Conn & Nelson, 2016). This idea comes from observations that *kai2* mutant phenotypes are opposite to the effects of karrikin treatment on wild-type plants, suggesting an endogenous signal is no longer perceived in *kai2*. Further support comes from the inconsistent availability of karrikins in the environment, the evolutionary conservation of KAI2 homologues throughout land plants, and the likely status of KAI2 as the ancestor of the strigolactone receptor in seed plants. Direct evidence for this postulated KAI2 ligand (KL), and therefore details on its chemical nature, are currently lacking.

In Arabidopsis, KAI2 does not appear to contribute to endogenous strigolactone perception and cannot functionally replace D14 (Waters *et al.*, 2015b). Likewise, D14 is unable to mediate responses to karrikins (Waters *et al.*, 2012). Nevertheless, KAI2 and D14 are able to respond to similar butenolide compounds, with substantial differences in ligand specificity depending on stereochemistry. To date, all reported naturally-occurring strigolactones contain a 2'*R*-configured butenolide ring with a methyl group at the 4' position. This arrangement originates in carlactone, the biosynthetic precursor for strigolactones and related compounds (Alder *et al.*, 2012; Yoneyama *et al.*, 2018). Accordingly, strigolactone analogues with a 2'*R* configuration (e.g. GR24^{5DS}) are most effective in activating D14-dependent processes (Scaffidi *et al.*, 2014; Villaécija-Aguilar *et al.*, 2019; Wang *et al.*, 2020; Zheng *et al.*, 2020). However, several studies have shown that strigolactone analogues with a butenolide ring in the non-natural, 2'*S*-configuration (e.g. GR24$^{ent\text{-}5DS}$) are active via KAI2 (Scaffidi *et al.*, 2014; Villaécija-Aguilar *et al.*, 2019; Wang *et al.*, 2020; Zheng *et al.*, 2020). Although the individual enantiomers of GR24 exhibit differential activity via KAI2 and D14, this enantiomer–receptor relationship is not strict (Scaffidi *et al.*, 2014; Villaécija-Aguilar *et al.*, 2019). Consequently, it is often difficult to distinguish whether the effects of GR24 and similar analogues occur through KAI2- or D14-dependent signalling. It would be highly desirable to find broadly effective, orthogonal ligands for KAI2 that exhibit minimal bioactivity via D14, and vice-versa. Deciphering the chemical features that improve ligand specificity will aid in the rational design of inhibitor compounds and may provide important clues about the identity and biosynthetic origins of KL.

Desmethyl strigolactone analogues, in which the 4' methyl group on the butenolide moiety is absent, are biologically inactive through D14 (Boyer *et al.*, 2012; de Saint Germain *et al.*, 2016). Previously, we observed that desmethyl-Yoshimulactone Green (dYLG), a desmethyl derivative of the fluorescent strigolactone analogue YLG, was much more active through Arabidopsis KAI2 than YLG itself (Yao *et al.*, 2018). Similarly, the desmethyl karrikin KAR_2 is more active than the methyl-substituted KAR_1 in Arabidopsis (Nelson *et al.*, 2010; Nelson *et al.*, 2011; Waters *et al.*, 2012; Waters *et al.*, 2015a; Fukui *et al.*, 2019). Here, we investigated further the relationship between methyl substituents on the butenolide moiety and bioactivity. We demonstrate that desmethyl butenolides in general are potent, rapid and specific agonists of KAI2 proteins from a wide taxonomic range of plants.

MATERIALS AND METHODS

Plant material

Arabidopsis thaliana mutants in L*er* background (*Atd14-1*, *kai2-2*, and *Atd14 kai2-2*) and transgenic Arabidopsis lines *KAI2pro:AtKAI2 S95A* and *KAI2pro:SmKAI2a*, both in the *kai2-2* (L*er*) background, were described previously (Waters *et al.*, 2015b). The *Marchantia polymorpha max2-1* mutant is described elsewhere (Mizuno *et al.*, 2020).

Hypocotyl elongation assays

Hypocotyl elongation assays were performed as described previously (Sun *et al.*, 2020).

Protein degradation assays

KAI2 and D14 degradation assays, protein extraction, electrophoresis and immunoblotting were performed as described previously (Sun *et al.*, 2020). Antibodies used were polyclonal anti-AtKAI2 (Waters *et al.*, 2015a), polyclonal AtD14 (Agrisera AS163694) and monoclonal anti-actin (Sigma A0480).

Transcript analysis

Arabidopsis seedlings were grown on solidified half-strength MS medium and transferred to liquid MS medium for treatment with butenolides, as described previously (Sun *et al.*, 2020).

For *Marchantia*, mature gemmae were arranged on a sterile wire mesh placed on half-strength B5 medium, and incubated under continuous white light at 20 °C for 24 h. By lifting the mesh, the gemmae were then floated on fresh liquid medium containing butenolides, and incubated for 6 h prior to harvesting. RNA extraction, DNase treatment, cDNA synthesis and quantitative PCR (qPCR) were performed as described previously for Arabidopsis (Sun *et al.*, 2020) and Marchantia (Mizuno *et al.*, 2020). Oligonucleotides are listed in Table S1.

Protein expression and purification

Molecular cloning, protein expression and protein purification of recombinant SUMO-AtKAI2, SUMO-AtKAI2 S95A, SUMO-AtD14 and SUMO-SmKAI2a were performed as described previously (Waters *et al.*, 2015b), except that affinity chromatography made use of TALON cobalt resin (Takara) for improved protein purity. The coding region from lysine 55 to tyrosine 318 of rice D14 (which omits the non-conserved Ser- and Gly-rich leader sequence; UniProtKB Q10A15) and the full-length coding region for rice KAI2 (UniProtKB Q10J20) were codon-optimized and synthesised (Genscript) before cloning into the *Bam*HI and *Xho*I sites of pE-SUMO-Amp (LifeSensors). An identical codon optimization and cloning strategy of full-length coding regions was performed for GmKAI2a (UniProtKB I1J9C0) and GmKAI2b (UniProtKB I1K2B0) from *Glycine max* (soybean). All proteins were expressed and purified in the same manner as the other SUMO-tagged proteins.

Yeast-2-hybrid

KAI2 and *D14* cDNA sequences were cloned into yeast expression vector pDEST-GBKT7 to generate BD-KAI2 and BD-D14, respectively. To make GAL4 DNA activation domain (AD) constructs, *SMAX1* and *SMXL7* cDNA sequences were cloned into yeast expression vector pDEST-GADT7. Detailed cloning procedures were described previously (Khosla *et al.*, 2020).

The yeast strain Y2H Gold (Clontech) was transformed by the lithium acetate-mediated method (Gietz & Woods, 2002). Co-transformed yeast strains were plated on SD/-Leu-Trp medium (Clontech) at 30 °C for 3 d. Interactions in yeast were tested on SD/-Leu-Trp-His and SD/-Leu-Trp-His-Ade (Clontech) media supplemented with *rac*-GR24, *rac*-dGR24, or 0.02% acetone control.

Differential scanning fluorimetry (DSF)

DSF was performed in 384-well format on a LightCycler 480 instrument (Roche) as described previously (Sun *et al.*, 2020).

Intrinsic tryptophan fluorescence (ITF)

ITF was performed in 384-well format on a BMG Labtech CLARIOstar multimode plate reader, using black microplates (Greiner 781076). Quadruplicate reactions (20 µL) contained 10 µM protein, 20 mM HEPES pH 7.5, 150 mM NaCl, 1.25% (v/v) glycerol, 5%, DMSO and 0-800 µM ligand. Ligands were diluted from DMSO stocks into buffer (20 mM HEPES pH 7.5, 150 mM NaCl, 1.25% (v/v) glycerol) at 2× concentration immediately before use, and then dispensed onto the plate with a multichannel pipette. A 2× solution of protein in buffer was prepared and then dispensed onto the plate using a repeat pipetter. The plate was mixed at 120 rpm for 2 mins, centrifuged at 500× *g* for 2 mins, and then incubated in the dark for 20 mins at room temperature. Fluorescence measurements were taken with either fixed wavelength filters (excitation 295/10 nm; longpass dichroic 325 nm; emission 360/20 nm) or with the LVF monochromator for emission scans (excitation 295/10 nm, emission 334-400 nm, step width 2 nm, emission bandwidth 8 nm). Measurements were performed at 25 °C using 20 flashes per well. Gain and focus settings were set empirically for each experimental run. Data were blank-corrected by subtraction of fluorescence values from an identical set of wells containing ligand but no protein. Data were imported into GraphPad Prism 8.1 where technical replicates were averaged. K_d values were estimated from untransformed fluorescence readings using nonlinear regression and the in-built "[Inhibitor] vs. response (three parameters)" model, with least squares regression as a fitting method and an asymmetrical (profile-likelihood) 95% confidence interval. The only constraint applied to the model was IC50 > 0. Data that yielded ambiguous fits and unstable parameters were reported as n.d. (not determinable).

Hydrolysis competition assays

Assays were conducted in triplicate in 96-well format on a BMG Labtech FLUOstar multimode plate reader, using black plates (Greiner 655900). Reactions contained 5 µM YLG or dYLG, 0–500 µM competitor, 1 µg protein, 100 mM HEPES, 150 mM NaCl and 0.1% DMSO (pH 7.5). The fluorescent hydrolysis substrate (5 mM YLG or dYLG) and the competitor ligand ($GR24^{5DS}$

or dGR24$^{ent\text{-}5DS}$, 10 to 50 mM; (*S*)-CN-deb or (*S*)-dCN-deb, 100 to 500 mM) were premixed to generate 1000× stocks in DMSO. These stocks were serially diluted with reaction buffer (100 mM HEPES, 150 mM NaCl, pH 7.5) to reach 1.11× working concentration. Proteins were diluted in buffer such that 10 µL of solution contained 1 µg of protein (0.1 mg/mL), and incubated on ice.

On ice, protein solution (10 µL) was dispensed with a repeat pipettor, followed by the addition of 90 µL substrate/competitor solution with a multichannel pipette. The plate was then loaded immediately onto the pre-warmed microplate reader, with the following measurement parameters: temperature 25 °C, excitation/emission: 485/520 mm; shaking for 3 seconds every 3 minutes, and 1% gain against the well with the highest initial fluorescence. Hydrolysis rate was defined as the change in fluorescence units over 15 minutes. Data were expressed relative to the hydrolysis activity in the absence of inhibitor. IC_{50} values were estimated in Graphpad Prism v.8 using nonlinear regression and the in-built "[Inhibitor] vs. response – variable slope (four parameters)" model, with least squares regression as a fitting method and an asymmetrical (profile-likelihood) 95% confidence interval.

Hydrolysis of GR24 and dGR24

Consumption of GR24 and dGR24 was monitored by HPLC as described previously (Waters *et al.*, 2015b) but with the following modifications: elution started at 0% acetonitrile:water, holding for 2 min and then increasing to 90% acetonitrile:water at 10 min; holding for 1.5 min and re-equilibrating for 3 min using a flow rate of 0.9 mL/min.

RESULTS

Arabidopsis responds to desmethyl butenolides via KAI2

We synthesised desmethyl-GR24 (dGR24) and desmethyl debranone (dCN-deb), which both lack the methyl group on the butenolide moiety (Figure S1). Both compounds were subsequently separated by chiral-phase HPLC into their respective enantiomers and stereochemistry was assigned on the basis of circular dichroism with reference to the methyl-substituted compounds (Figure S1).

We tested the ability of each desmethyl enantiomer to inhibit Arabidopsis hypocotyl elongation, relative to their methyl-substituted counterparts. dGR24^{5DS} had no detectable activity in WT L*er*, whereas GR24^{5DS} was effective (Figure 1A). This response to GR24^{5DS} was mediated primarily by AtD14, but also by KAI2 to a limited degree as previously reported (Scaffidi *et al.*, 2014; Villaécija-Aguilar *et al.*, 2019). By contrast, dGR24$^{ent\text{-}5DS}$ yielded a similar response to GR24$^{ent\text{-}5DS}$ in L*er* seedlings. However, the response to dGR24$^{ent\text{-}5DS}$ was entirely KAI2-dependent (Figure 1A). Among the debranone analogues, (*S*)-CN-deb and (*S*)-dCN-deb were the only compounds to elicit a hypocotyl response, although (*S*)-CN-deb was the more active of the two in this assay (Figure 1B). As with dGR24$^{ent\text{-}5DS}$, (*S*)-dCN-deb was only active via KAI2.

We reasoned that the hypocotyl elongation assay, which involves measuring seedling growth more than a week after seeds are first exposed to the active compound, may be too indirect and protracted to study more nuanced effects of butenolide methyl status on bioactivity. Having determined that desmethyl butenolides act solely through KAI2, we compared the efficacy of methyl and desmethyl butenolides in KAI2 degradation assays, which reveal the direct effect of butenolides on the receptor protein itself (Waters *et al.*, 2015a). KAR_2 was more than five times as potent as KAR_1 in promoting KAI2 degradation, as observed previously (Waters *et al.*, 2015a; Yao *et al.*, 2018), while dGR24$^{ent\text{-}5DS}$ was the most effective of all compounds examined (Figure 1C). In a direct comparison of GR24$^{ent\text{-}5DS}$ and dGR24$^{ent\text{-}5DS}$, the latter was approximately 10-fold more active at stimulating KAI2 degradation (Figure 1D). We also found that dGR24$^{ent\text{-}5DS}$ and (*S*)-dCN-deb only induced degradation of KAI2 and not of D14, the latter of which did not respond robustly to any of the compounds examined under our experimental conditions (Figure 1E). Furthermore, we found that *rac*-dGR24 was able to enhance a two-hybrid interaction between Arabidopsis KAI2 and SMAX1 expressed in yeast, whereas the interaction between D14 and SMXL7 was only responsive to *rac*-GR24 (Figure 1F).

To gain further insight into the kinetics of butenolide response on a short timescale, we measured the induction of *DLK2* transcripts, which are sensitive to both KAI2- and D14-dependent signalling pathways (Waters *et al.*, 2012). Among the two pairs of GR24 and dGR24 enantiomers, we found that dGR24$^{ent\text{-}5DS}$ was the most effective inducer of *DLK2* in L*er*, although there was a 5-fold induction by the other three compounds as well (Figure 2A). The

12-fold induction of *DLK2* expression by dGR24$^{ent\text{-}5DS}$ was absent in *kai2-2* mutants, indicating that KAI2 alone mediates response to this compound. Although GR24^{5DS} and GR24$^{ent\text{-}5DS}$ largely acted through AtD14 and KAI2 respectively, there was some evidence of weak activity through the non-preferred signalling receptor (e.g. GR24$^{ent\text{-}5DS}$ via AtD14), as has been reported previously for *DLK2* induction (Scaffidi *et al.*, 2014). We found that dGR24$^{ent\text{-}5DS}$ was consistently more active than similar concentrations of GR24$^{ent\text{-}5DS}$ across a 100-fold concentration range in L*er* seedlings (Figure 2B). Unexpectedly, we found that dGR24$^{ent\text{-}5DS}$ induced a faster but more transient increase in *DLK2* transcripts compared to GR24$^{ent\text{-}5DS}$. *DLK2* expression peaked at 2 h after dGR24$^{ent\text{-}5DS}$ treatment and decreased thereafter; by contrast, the response to GR24$^{ent\text{-}5DS}$ rose slowly over the 8-h time course (Figure 2C). Overall patterns were similar for the comparison of (*S*)-CN-deb and (*S*)-dCN-deb: again, the desmethyl debranone was KAI2-specific (Figure 2D) and showed greater potency than its methyl-substituted counterpart (Figure 2E). The transient induction of *DLK2* transcripts was particularly pronounced for (*S*)-dCN-deb (Figure 2F). These results indicate that desmethyl butenolides uniquely activate KAI2, and do so with greater efficacy than their methyl-substituted counterparts. In addition, as with methyl butenolides, the stereochemical configuration of the O-linked butenolide ring influences the bioactivity of desmethyl analogues.

KAI2 and D14 have opposite preferences for desmethyl and methyl butenolides *in vitro*

Both KAI2 and D14 proteins are thermally destabilised in the presence of GR24, as revealed by differential scanning fluorimetry (DSF) or thermal shift assays (Hamiaux *et al.*, 2012; Abe *et al.*, 2014; Waters *et al.*, 2015b). In addition, the affinity of the ligand-receptor relationship can be inferred using intrinsic tryptophan fluorescence (ITF) measurements, in which ligand binding alters the tryptophan microenvironment and thus the overall fluorescent properties of the protein (Ghisaidoobe & Chung, 2014). ITF measurements are only appropriate for ligands that do not interfere with a fluorescence signal from tryptophan, and ITF has been used elsewhere to infer a ligand-binding relationship between strigolactone analogues such as GR24 and various D14 and KAI2 homologues (de Saint Germain *et al.*, 2016; de Saint Germain *et al.*, 2020). ITF data has also been documented as evidence for binding of KAR_1 by

KAI2 (Toh *et al.*, 2014), but we contend that karrikins are incompatible with ITF assays because they absorb strongly in the same wavelengths (280-295 nm) that excite tryptophan (Figure S2).

Ligand-induced responses in both DSF and ITF may indicate a change in protein conformation associated with ligand binding and/or hydrolysis. We examined the response of SUMO-tagged KAI2 and D14 proteins from Arabidopsis and rice to the same enantiomers of methyl and desmethyl butenolides that were tested in Arabidopsis hypocotyl elongation assays. The N-terminal 6xHIS-SUMO tag is used to aid expression in *E. coli* and does not interfere with ligand-induced thermal instability or enzymatic function of the downstream receptor-hydrolase (Sun *et al.*, 2020). All purified proteins described in assays hereafter included the 6xHIS-SUMO tag.

Both AtKAI2 and OsKAI2 proteins responded robustly to the bioactive enantiomers dGR24$^{ent\text{-}5DS}$ and (*S*)-dCN-deb in DSF assays, but showed comparatively weak responses to their methyl-substituted counterparts under the same conditions (Figure 3A; Figure S3A). The destabilisation of AtKAI2 was particularly pronounced, showing discernible response to concentrations of desmethyl ligands above 10 µM, which is half the concentration of protein in the assay, whereas OsKAI2 required 100 µM ligand for a clear destabilisation response. In ITF assays, saturation of fluorescence was achieved for both KAI2 proteins in response to desmethyl butenolides at 100 to 200 µM and above, but saturation was not reached for either of the methyl-substituted variants with either AtKAI2 or OsKAI2 (Figure 3C; Figure S3C). The enhanced DSF response to desmethyl butenolides of AtKAI2 relative to OsKAI2 was reflected by the smaller K_d value inferred from ITF assays (e.g. ~10 µM vs. 73 µM for dGR24$^{ent\text{-}5DS}$), which indicates that AtKAI2 had a somewhat higher affinity for these ligands compared to OsKAI2. K_d values could not be calculated for the methyl-substituted ligands as saturation of response was not reached. We also examined the response of KAI2 proteins to the non-bioactive *R*-configured enantiomers, and found that both AtKAI2 and OsKAI2 responded to dGR24^{5DS}, although with less sensitivity than to the bioactive dGR24$^{ent\text{-}5DS}$ and with qualitatively different melt profiles (Figure S4A). This change in melt profile might indicate that the two enantiomers of dGR24 induce slightly different protein conformational shifts. Responses of both AtKAI2 and OsKAI2 to (*R*)-dCN-deb were negligible, in stark contrast to (*S*)-dCN-deb (Figure S4B). Finally, we also found that two KAI2 orthologues from soybean (*Glycine max*) responded much more prominently to dGR24$^{ent\text{-}5DS}$ than GR24$^{ent\text{-}5DS}$ (Figure S5), further suggesting that

the preference of KAI2 proteins for desmethyl butenolides might be widespread among angiosperms.

Because the plant responses to desmethyl butenolides were KAI2-specific, we also assessed the response of AtD14 and OsD14 to the same panel of methyl and desmethyl compounds. In DSF assays, both AtD14 and OsD14 responded clearly to the biologically-active GR24^{5DS}, and AtD14 responded to (*S*)-CN-deb; however, responses to the corresponding desmethyl enantiomers were negligible (Figure 3B; Figure S3B). In ITF assays, saturable responses were only observed for AtD14 and OsD14 with GR24^{5DS}, but there was evidence of appreciable fluorescence suppression with dGR24^{5DS} as well (Figure 3D; Figure S3D). AtD14 and OsD14 both responded in DSF assays to the less-preferred *S*-configured GR24$^{ent\text{-}5DS}$, but both showed a comparatively weak response to dGR24$^{ent\text{-}5DS}$ with no clear T_m shift (Figure S6). Likewise, both proteins responded to (*R*)-CN-deb but not to (*R*)-dCN-deb, even though neither of these compounds is bioactive in Arabidopsis hypocotyl elongation assays (Figure S6). Therefore, irrespective of stereochemistry, D14 proteins only exhibit thermal instability in response to compounds with a methyl-substituted butenolide group. Taken together with the plant activity data, and assuming that thermal destabilisation is a consequence of receptor activation, these results suggest that only methyl butenolides, and not desmethyl equivalents, are capable of activating D14 proteins. However, the suppression of D14 tryptophan fluorescence by dGR24^{5DS} indicates that D14 is capable of interacting with this desmethyl compound, even if it is biologically inactive.

We next considered whether butenolide methyl status affected the enzymatic activity of AtKAI2 and AtD14, using the optimal enantiomers for each protein based on bioactivity. We found that AtKAI2 hydrolysed dGR24$^{ent\text{-}5DS}$ ~2.5 times faster than GR24$^{ent\text{-}5DS}$ over a six-hour incubation (Figure 4A). Unexpectedly, AtD14 showed very strong hydrolysis activity towards dGR24^{5DS}, with ~5-fold greater initial hydrolysis rate of dGR24^{5DS} over GR24^{5DS} (Figure 4B). Hydrolysis of the fluorogenic substrate desmethyl-Yoshimulactone Green (dYLG) by AtKAI2 was efficiently inhibited by dGR24$^{ent\text{-}5DS}$ and (*S*)-dCN-deb, yielding IC_{50} values similar to the K_d values derived from ITF assays (Figure 4C, E). Crucially, dYLG hydrolysis by AtKAI2 was unaffected by the methyl-substituted competitors. However, AtD14-dependent hydrolysis of YLG, which contains a methyl-butenolide moiety, was inhibited to similar degrees by both desmethyl and methyl-substituted butenolide competitors (Figure 4D, F). Coupled with the

very fast direct hydrolysis of dGR24^{5DS} by AtD14, this result further supports the interpretation that AtD14 can bind and hydrolyse desmethyl butenolides, even though these compounds are non-bioactive through D14.

The Atkai2 S95A mutant reveals ligand-induced receptor dynamics

The catalytic S95A mutant of AtKAI2 is non-functional *in planta*, cannot hydrolyse GR24$^{ent\text{-}5DS}$, and does not respond to GR24$^{ent\text{-}5DS}$ in DSF assays (Waters *et al.*, 2015b; Yao *et al.*, 2018). Unsurprisingly, we found that the hydrolase function is also necessary for hydrolysis of dYLG, and for plant responses to dGR24$^{ent\text{-}5DS}$ at least in terms of seedling hypocotyl elongation (Figure S7A, B). However, in DSF assays we noticed that Atkai2 S95A responded to dGR24$^{ent\text{-}5DS}$ with progressive decreases in melting temperature, from ~43 °C to ~41 °C, as ligand concentration increased (Figure S7C). This shift in melting profile was not observed with GR24$^{ent\text{-}5DS}$, and was qualitatively different from that observed in the wild-type protein, in which the melting point shifts from approximately 44 °C to a substantially lower temperature with a broader range of 32-37 °C (Figure 3A). In ITF assays, dGR24$^{ent\text{-}5DS}$ suppressed the fluorescence of Atkai2 S95A in a ligand concentration-dependent manner, but no discernible response was seen with GR24$^{ent\text{-}5DS}$ (Figure S7D-F). Like with DSF, the response to dGR24$^{ent\text{-}5DS}$ was muted compared with the wild type protein (Figure 3C) and did not saturate at 400 µM dGR24$^{ent\text{-}5DS}$. These results indicate that although incapable of hydrolysing or mediating biological responses to desmethyl butenolides, the S95A variant retains some elements of ligand-dependent conformational change. By combining a highly active ligand with a functionally inactive receptor, our experiments may have captured the relatively moderate initial effects of ligand binding on KAI2 conformation, and separated them from the much more dramatic consequences of receptor activation following ligand hydrolysis.

KAI2 preference for desmethyl butenolides is evolutionarily ancient

Previously we identified from the lycophyte fern *Selaginella moellendorffii* the KAI2 orthologue SmKAI2a, which was able to partially complement the *Atkai2-2* seedling hypocotyl phenotype (Waters *et al.*, 2015b). However, neither karrikins, GR24$^{ent\text{-}5DS}$ nor carlactone could elicit any biological response in *KAI2pro:SmKAI2a* Arabidopsis transgenics, suggesting that none of these compounds are capable of activating SmKAI2a (Waters 2015). Nevertheless,

the partial phenotypic complementation implied that SmKAI2a could mediate responses to KL and perhaps other exogenous butenolides. We first considered whether SmKAI2a would respond to dGR24$^{ent\text{-}5DS}$ in DSF assays, and found that it responded robustly at 25 µM and above but was non-responsive to GR24$^{ent\text{-}5DS}$ even at 200 µM (Figure 5A). This result was mirrored in ITF assays (Figure 5B). We next tested whether dGR24$^{ent\text{-}5DS}$ could activate SmKAI2a expressed in Arabidopsis. Although hypocotyl lengths of *KAI2pro:SmKAI2a* transgenic seedlings were not affected by dGR24$^{ent\text{-}5DS}$ at concentrations up to 1 µM (Figure 5C), we did observe that *DLK2* transcripts responded positively at 10 µM (Figure 5D). With a 2.5-fold increase in steady-state *DLK2* transcript levels relative to mock-treated controls, the response in *SmKAI2a* transgenics was substantially weaker than that observed in WT Arabidopsis L*er* seedlings (~20-fold). However, this difference is consistent with the partial phenotypic complementation characteristic of these lines, which presumably reflects the evolutionary distance between *Selaginella* and Arabidopsis and incompatibility with interacting proteins such as SMAX1 or MAX2 (Waters *et al.*, 2015b). Accordingly, we conclude that SmKAI2a is able to mediate weak responses to dGR24$^{ent\text{-}5DS}$ both *in vitro* and in a heterologous expression system.

Arabidopsis and *S. moellendorffii* are both vascular plants belonging to lineages that diverged 400-430 mya (Bowman, 2013). To assess whether a preference for desmethyl butenolides likely existed in the earliest land plants, we examined the transcriptional response of gemmae of the liverwort *Marchantia polymorpha* to individual enantiomers of GR24 and dGR24. We measured the abundance of transcripts corresponding to *DIENE LACTONE HYDROLASE-LIKE PROTEIN 1* (*DLP1*; Mapoly0095s0043), whose expression is regulated in a *MpMAX2*-dependent manner (Figure S8). We found that treatment of WT gemmae with 1 µM dGR24$^{ent\text{-}5DS}$ resulted in a five-fold increase in *DLP1* transcripts, which was approximately twice the response observed with GR24$^{ent\text{-}5DS}$ (Figure 5E). In addition, the 2'*R*-oriented enantiomers induced a consistently weaker *DLP1* response relative to their 2'*S* counterparts, and the *Mpmax2-1* mutant was fully insensitive to all compounds examined (Figure 5E). Both of these observations are consistent with the *DLP1* response being mediated by MpKAI2a and/or MpKAI2b, which are the two KAI2 homologues in this species (Waters *et al.*, 2015b; Mizuno *et al.*, 2020). Overall, these results suggest that the preference of KAI2 orthologues for

desmethyl butenolides over methyl-substituted butenolides was present in the common ancestor of all land plants.

DISCUSSION

This work establishes that desmethyl butenolides are preferred substrates for diverse KAI2 homologues, while presenting no detectable bioactivity via D14 homologues. Although karrikins are also KAI2-specific plant growth regulators, they are inactive *in vitro* (Waters *et al.*, 2015a; Waters *et al.*, 2015b; Yao *et al.*, 2018; Fukui *et al.*, 2019; Sun *et al.*, 2020), do not appear to be active in all plants (Flematti *et al.*, 2011; Hoffmann *et al.*, 2014) and have slower and less sensitive activation kinetics *in vivo* compared to GR24$^{ent\text{-}5DS}$ (Wang *et al.*, 2020). Considering that the preferences of KAI2 and D14 for the two GR24 enantiomers are not always absolute (Scaffidi *et al.*, 2014; Villaécija-Aguilar *et al.*, 2019), we propose that desmethyl butenolide compounds can be used to selectively and potently activate KAI2-dependent signalling, independently of strigolactone signalling, in a range of species and assays.

We found that AtD14 hydrolysed the non-bioactive compound dGR24^{5DS} at a considerably faster rate than GR24^{5DS}, which is bioactive. This result is consistent with earlier findings that compared the hydrolysis activity of D14 towards YLG and dYLG (Yao *et al.*, 2018) and RMS3 (the pea orthologue of D14) towards other fluorogenic substrates with methyl-substituted (*rac*-GC242) and desmethyl (*rac*-GC486) butenolide groups (de Saint Germain *et al.*, 2016). Despite these favourable hydrolysis rates, dGR24^{5DS} and *rac*-GC486 are nevertheless unable to induce a substantial conformational change in the receptor structure as judged by DSF (Figure 3; Supplemental Figure 3; (de Saint Germain *et al.*, 2016). With bioactive compounds such as *rac*-GR24 and *rac*-GC242, the kinetic mechanism of D14 involves the formation of a stable intermediate, derived from the butenolide ring, covalently bound to the catalytic histidine (de Saint Germain *et al.*, 2016; Yao *et al.*, 2016). The fast hydrolysis rates of desmethyl butenolides by D14 may result from the lack of formation of this reaction intermediate, which normally might be expected to slow down the rate of hydrolysis. By extension, it is likely that the His-modified intermediate corresponds to the protein conformational change revealed by DSF and, ultimately, the activated state of the receptor.

The fact that D14 can hydrolyse and therefore inactivate desmethyl butenolides may account in part for their apparently transient bioactive period (Figure 2). However, this is not likely to be the complete explanation because *Atd14* seedlings retained a noticeable transient peak in levels of *DLK2* transcripts upon treatment with (*S*)-dCN-deb (Figure 2F). We speculate that this transient induction of *DLK2* transcripts may reflect very rapid activation and subsequent turnover of KAI2 by desmethyl butenolides that exceeds the capacity of the cell to regenerate fresh receptors through protein synthesis. Alternatively, increased levels of DLK2 protein might contribute to the hydrolysis and inactivation of desmethyl butenolides: DLK2 is a relatively recent paralogue of D14 that also possesses hydrolase activity and, tentatively, may negatively regulate some aspects of KAI2-dependent signalling over different timescales (Waters *et al.*, 2015b; Végh *et al.*, 2017; Ho-Plágaro *et al.*, 2020).

Serendipitously, the AtKAI2 S95A mutant protein provides insight into how desmethyl butenolides are preferred by KAI2. Independent of hydrolytic activity, AtKAI2 S95A showed clear evidence of binding dGR24$^{ent\text{-}5DS}$ but no sign of interaction with GR24$^{ent\text{-}5DS}$. This result implies that a butenolide methyl group negatively influences the binding affinity to KAI2, which must explain in part why desmethyl butenolides are more active. Evidently, methyl-substituted butenolides are active with KAI2, albeit less so than desmethyl butenolides, which implies that there is sufficient flexibility in the active site of KAI2 to accommodate both types of ligand. Given the range of molecular sizes of active compounds, it seems unlikely that a single methyl group should inhibit binding and bioactivity by restricting access to the active site. Instead, perhaps the methyl group influences the orientation of the butenolide carbonyl oxygen relative to the catalytic serine. For D14, the butenolide methyl group seems to prevent "futile" hydrolysis. Perhaps this rapid hydrolysis results from misalignment of the butenolide ring with the other catalytic residues, such that the reaction intermediates are too short-lived to support receptor activation. In the case of KAI2, the lack of a methyl group enhances both the rate of hydrolysis (Figure 4) and the activation of the receptor, possibly because of a more favourable orientation for nucleophilic attack and formation of the covalently-linked reaction intermediates. In addition, we found that an *S*-configured butenolide ring remains important for activity via KAI2, irrespective of the loss of the butenolide methyl group, since dGR24$^{ent\text{-}5DS}$ was much more active than dGR24^{5DS}, and a similar trend was observed for (*S*)-dCN-deb versus (*R*)-dCN-deb. This finding further lends support to the importance of precise substrate

orientation in the active site for optimal rates of receptor activation and thus sensitivity for signalling.

Another outcome of experiments with the AtKAI2 S95A variant was the ability to distinguish between the signals due to ligand binding and those due to receptor activation. Because the responses of AtKAI2 S95A to dGR24$^{ent\text{-}5DS}$ were less extreme than the responses of WT AtKAI2 and because AtKAI2 S95A is non-functional *in vivo*, we infer that ligand binding alone is insufficient for receptor activation, at least when the catalytic triad is disrupted. Furthermore, we conclude that the majority of the signals detected in DSF and ITF assays with WT AtKAI2 result from a substantial, destabilising conformational shift associated with receptor activation, and this shift requires an intact catalytic triad. Based on how D14 behaves (Yao *et al.*, 2016), this large change presumably involves partial unfolding of the lid domain, which is consistent with a decrease in overall melting temperature reported by DSF. Nevertheless, both DSF and ITF assays showed a noticeable response of AtKAI2 S95A to dGR24$^{ent\text{-}5DS}$. We interpret this as the moderate effect on the protein structure associated specifically with ligand binding. This is reminiscent of the minor conformational changes reported when comparing the apo structure with a ligand-bound structure for both KAI2 and D14 (Guo *et al.*, 2013; Zhao *et al.*, 2015). Molecular dynamics simulations have also suggested that a similar minor conformational change is induced by ligand binding and leads to a slightly increased pocket volume to accommodate the ligand in the optimal position (Bürger & Chory, 2020a). It is possible that the large conformational changes associated with receptor activation are only observable in solution, because this form is too intrinsically disordered to undergo crystallisation. However, if there is a suitable second protein partner (e.g. MAX2/D3) present to stabilise the active state of the receptor, then this state may be successfully captured under crystallisation conditions (Yao *et al.*, 2016; Shabek *et al.*, 2018). In general, bioactivity corresponded well with receptor activation revealed by DSF: no *S*-configured bioactive compound failed to destabilise KAI2 proteins. However, the *R*-configured non-bioactive dGR24^{5DS} resulted in some destabilisation of AtKAI2 and, to a lesser extent, OsKAI2 (Supplemental Figure 4). It could be the case that opposite ligand stereoconfigurations induce slightly different conformational changes that both result in thermal destabilisation. However, perhaps only specific conformational changes are able to trigger the protein-protein interactions that are necessary for signalling in plants.

Strigolactones exuded into soil stimulate growth of arbuscular mycorrhizal (AM) fungi and promote the formation of symbiotic interactions between plant roots and AM fungi (Akiyama *et al.*, 2005; Besserer *et al.*, 2006). Recent evidence shows that desmethyl butenolides affect the growth of the model AM fungus *Rhizophagus irregularis* and enhance its capacity to invade *Medicago truncatula* roots (Taulera *et al.*, 2020). Taulera *et al*. (2020) used *rac*-2'-*epi*-dGR24, a racemic mixture of two 2' epimers of dGR24 (dGR24^{4DO} and dGR24$^{ent\text{-}4DO}$), and therefore we cannot be certain that these epimers activate KAI2 in the same way as dGR24$^{ent\text{-}5DS}$. Nevertheless, *rac*-2'-*epi*-dGR24 was shown to enhance root invasion by the fungus similarly to *rac*-GR24. Considering that KAI2 is required for successful AM symbiosis in rice (Gutjahr *et al.*, 2015), this result might be interpreted as evidence that dGR24 creates a permissive state in the plant root for fungal entry by activating KAI2. Interestingly, *rac*-2'-*epi*-dGR24 had opposite effects to *rac*-GR24 on *R. irregularis* germ tube growth and branching (Taulera *et al.*, 2020), which may suggest that desmethyl butenolides are inhibitors competing with strigolactones for access to the same fungal receptor. In light of our results, it would be desirable to repeat such assays with the specific stereoisomer known to activate KAI2, namely dGR24$^{ent\text{-}5DS}$, which we would predict to be more active.

The discovery that desmethyl butenolides are strong elicitors of KAI2 has implications for the identity of KL. First, and as inferred previously (Scaffidi *et al.*, 2013), it is consistent with KL having a biosynthetic origin that is independent of carlactone and its strigolactone derivatives, which all possess a methyl-substituted butenolide ring. It is conceivable that there exists an endogenous enzyme with strigolactone demethylase activity to generate KL. However, the preferred 2'(*S*) stereochemistry of KAI2 ligands is opposite to that of natural strigolactones, and natural strigolactone-like compounds with a desmethyl D-ring have yet to be reported, even though such compounds would likely be discovered via seed germination bioassays (de Saint Germain *et al.*, 2020). Furthermore, there has been evolutionary loss of key enzymes in strigolactone biosynthesis (e.g. CCD8 and MAX1 in *Marchantia polymorpha*; MAX1 in *Physcomitrella patens*) but no reported loss of KAI2 signalling components across the land plants (Walker *et al.*, 2019), which suggests that KAI2-dependent signalling does not necessarily require a strigolactone derivative. Second, the finding that KAI2-dependent signalling and/or KAI2 homologues from *Marchantia*, *Selaginella*, soybean, rice and Arabidopsis all exhibit a preference for desmethyl butenolides would indicate that KL itself,

and not just KAI2, is evolutionarily ancient and structurally conserved. Accordingly, we predict that KL is a desmethyl butenolide compound, most probably connected to a hydrophobic electron-withdrawing leaving group.

Our findings also will help in the rational design of further KAI2-specific activators or inhibitors. As the germination of root parasitic weed seeds in the Orobanchaceae is regulated by KAI2/HTL-type receptors, this knowledge will be particularly pertinent for approaches to control these weeds. Several species within the Orobanchaceae have undergone considerable expansion of the *KAI2*/*HTL* receptor gene family (Conn *et al.*, 2015; Tsuchiya *et al.*, 2015). Although many parasitic KAI2s appear to have developed a strong preference for methyl-substituted butenolides (i.e. host strigolactones; (Uraguchi *et al.*, 2018; de Saint Germain *et al.*, 2020)), it is possible that a cocktail of stimulants that target a broad range of receptors simultaneously – including the "conserved" KAI2c clade thought to be specific for KL (Conn & Nelson, 2016) – will enhance the overall efficacy of treatments for clearing the soil seed bank.

ACKNOWLEDGEMENTS

We gratefully acknowledge funding support from the Australian Research Council (FT150100162 to MTW; DP160102888 to GRF and MTW), a Fellowship Support grant from the University of Western Australia to MTW, and the National Science Foundation (IOS-1740560 and IOS-1856741 to DCN). YM was the recipient of a joint PhD scholarship from the China Scholarship Council.

AUTHOR CONTRIBUTIONS

MTW, JY, AS, and GRF designed experiments. MTW, JY, AS, YM, KTM, AKo and AKh conducted the experiments. MTW, JY, JK, DCN, and GRF analysed and interpreted the data. MTW wrote the manuscript with feedback from all authors.

DATA AVAILABILITY

The data that support the findings of this study are available from the corresponding author upon reasonable request.

REFERENCES

Abe S, Sado A, Tanaka K, Kisugi T, Asami K, Ota S, Kim HI, Yoneyama K, Xie X, Ohnishi T, et al. 2014. Carlactone is converted to carlactonoic acid by MAX1 in Arabidopsis and its methyl ester can directly interact with AtD14 in vitro. *Proceedings of the National Academy of Sciences* **111**(50): 18084-18089.

Akiyama K, Matsuzaki K-i, Hayashi H. 2005. Plant sesquiterpenes induce hyphal branching in arbuscular mycorrhizal fungi. *Nature* **435**(7043): 824.

Al-Babili S, Bouwmeester HJ. 2014. Strigolactones, a Novel Carotenoid-Derived Plant Hormone. *Annual Review of Plant Biology* **66**(1): 1-26.

Alder A, Jamil M, Marzorati M, Bruno M, Vermathen M, Bigler P, Ghisla S, Bouwmeester H, Beyer P, Al-Babili S. 2012. The Path from β-Carotene to Carlactone, a Strigolactone-Like Plant Hormone. *Science* **335**(6074): 1348-1351.

Besserer A, Puech-Pagès V, Kiefer P, Gomez-Roldan V, Jauneau A, Roy S, Portais J-C, Roux C, Bécard G, Séjalon-Delmas N. 2006. Strigolactones Stimulate Arbuscular Mycorrhizal Fungi by Activating Mitochondria. *PLoS Biology* **4**(7): e226.

Bowman JL. 2013. Walkabout on the long branches of plant evolution. *Current Opinion in Plant Biology* **16**(1): 70-77.

Boyer F-D, Germain AdS, Pillot J-P, Pouvreau J-B, Chen VX, Ramos S, Stévenin A, Simier P, Delavault P, Beau J-M, et al. 2012. Structure-Activity Relationship Studies of Strigolactone-Related Molecules for Branching Inhibition in Garden Pea: Molecule Design for Shoot Branching. *Plant Physiology* **159**(4): 1524-1544.

Bunsick M, Toh S, Wong C, Xu Z, Ly G, McErlean CSP, Pescetto G, Nemrish KE, Sung P, Li JD, et al. 2020. SMAX1-dependent seed germination bypasses GA signalling in Arabidopsis and Striga. *Nature Plants*: 1-7.

Bürger M, Chory J. 2020a. In-silico analysis of the strigolactone ligand-receptor system. *Plant Direct* **4**(9): e00263.

Bürger M, Chory J. 2020b. The Many Models of Strigolactone Signaling. *Trends in Plant Science*.

Bürger M, Mashiguchi K, Lee HJ, Nakano M, Takemoto K, Seto Y, Yamaguchi S, Chory J. 2019. Structural Basis of Karrikin and Non-natural Strigolactone Perception in Physcomitrella patens. *Cell Reports* **26**(4): 855-865.e855.

Bythell-Douglas R, Rothfels CJ, Stevenson DWD, Graham SW, Wong GK-S, Nelson DC, Bennett T. 2017. Evolution of strigolactone receptors by gradual neo-functionalization of KAI2 paralogues. *BMC Biology* **15**(1): 52.

Carbonnel S, Das D, Varshney K, Kolodziej MC, Villaécija-Aguilar JA, Gutjahr C. 2020. The karrikin signaling regulator SMAX1 controls Lotus japonicus root and root hair development by suppressing ethylene biosynthesis. *Proceedings of the National Academy of Sciences*: 202006111.

Chesterfield RJ, Whitfield JH, Pouvreau B, Cao D, Alexandrov K, Beveridge CA, Vickers CE. 2020. Rational Design of Novel Fluorescent Enzyme Biosensors for Direct Detection of Strigolactones. *ACS synthetic biology*.

Choi J, Lee T, Cho J, Servante EK, Pucker B, Summers W, Bowden S, Rahimi M, An K, An G, et al. 2020. The negative regulator SMAX1 controls mycorrhizal symbiosis and strigolactone biosynthesis in rice. *Nature Communications* **11**(1): 2114.

Conn CE, Bythell-Douglas R, Neumann D, Yoshida S, Whittington B, Westwood JH, Shirasu K, Bond CS, Dyer KA, Nelson DC. 2015. Convergent evolution of strigolactone perception enabled host detection in parasitic plants. *Science* **349**(6247): 540-543.

Conn CE, Nelson DC. 2016. Evidence that KARRIKIN-INSENSITIVE2 (KAI2) Receptors may Perceive an Unknown Signal that is not Karrikin or Strigolactone. *Frontiers in Plant Science* **6**: 1219.

de Saint Germain A, Clavé G, Badet-Denisot M-A, Pillot J-P, Cornu D, Caer J-PL, Burger M, Pelissier F, Retailleau P, Turnbull C, et al. 2016. An histidine covalent receptor and butenolide complex mediates strigolactone perception. *Nature Chemical Biology* **12**(10): 787-794.

de Saint Germain A, Jacobs A, Brun G, Pouvreau J-B, Braem L, Cornu D, Clavé G, Baudu E, Steinmetz V, Servajean V, et al. 2020. A Phelipanche ramosa KAI2 Protein Perceives enzymatically Strigolactones and Isothiocyanates. *bioRxiv*: 2020.2006.2009.136473.

Delaux PM, Xie X, Timme RE, Puech-Pages V, Dunand C, Lecompte E, Delwiche CF, Yoneyama K, Bécard G, Séjalon-Delmas N. 2012. Origin of strigolactones in the green lineage. *New Phytologist* **195**(4): 857-871.

Flematti GR, Ghisalberti EL, Dixon KW, Trengove RD. 2004. A compound from smoke that promotes seed germination. *Science* **305**(5686): 977.

Flematti GR, Goddard-Borger ED, Merritt DJ, Ghisalberti EL, Dixon KW, Trengove RD. 2007. Preparation of 2H-Furo[2,3-c]pyran-2-one Derivatives and Evaluation of Their Germination-Promoting Activity. *Journal of Agricultural and Food Chemistry* **55**(6): 2189-2194.

Flematti GR, Merritt DJ, Piggott MJ, Trengove RD, Smith SM, Dixon KW, Ghisalberti EL. 2011. Burning vegetation produces cyanohydrins that liberate cyanide and stimulate seed germination. *Nature Communications* **2**(1): 360.

Fukui K, Arai K, Kasahara H, Asami T, Hayashi K-i. 2019. Synthetic agonist of HTL/KAI2 shows potent stimulating activity for Arabidopsis seed germination. *Bioorganic & Medicinal Chemistry Letters* **29**(17): 2487-2492.

Ghisaidoobe ABT, Chung SJ. 2014. Intrinsic Tryptophan Fluorescence in the Detection and Analysis of Proteins: A Focus on Förster Resonance Energy Transfer Techniques. *International Journal of Molecular Sciences* **15**(12): 22518-22538.

Gietz RD, Woods RA. 2002. Transformation of yeast by lithium acetate/single-stranded carrier DNA/polyethylene glycol method. *Methods in Enzymology* **350**: 87-96.

Guo Y, Zheng Z, Clair JJL, Chory J, Noel JP. 2013. Smoke-derived karrikin perception by the α/β-hydrolase KAI2 from Arabidopsis. *Proceedings of the National Academy of Sciences* **110**(20): 8284-8289.

Gutjahr C, Gobbato E, Choi J, Riemann M, Johnston MG, Summers W, Carbonnel S, Mansfield C, Yang S-Y, Nadal M, et al. 2015. Rice perception of symbiotic arbuscular mycorrhizal fungi requires the karrikin receptor complex. *Science* **350**(6267): 1521-1524.

Hamiaux C, Drummond Revel SM, Janssen Bart J, Ledger Susan E, Cooney Janine M, Newcomb Richard D, Snowden Kimberley C. 2012. DAD2 Is an α/β Hydrolase Likely to Be Involved in the Perception of the Plant Branching Hormone, Strigolactone. *Current Biology* **22**(21): 2032-2036.

Ho-Plágaro T, Morcillo RJL, Tamayo-Navarrete MI, Huertas R, Molinero-Rosales N, López-Ráez JA, Macho AP, García-Garrido JM. 2020. DLK2 regulates arbuscule hyphal branching during arbuscular mycorrhizal symbiosis. *New Phytologist*.

Hoffmann B, Proust H, Belcram K, Labrune C, Boyer F-D, Rameau C, Bonhomme S. 2014. Strigolactones Inhibit Caulonema Elongation and Cell Division in the Moss Physcomitrella patens. *PLoS ONE* **9**(6): e99206.

Jiang L, Liu X, Xiong G, Liu H, Chen F, Wang L, Meng X, Liu G, Yu H, Yuan Y, et al. 2013. DWARF 53 acts as a repressor of strigolactone signalling in rice. *Nature* **504**(7480): 401.

Khosla A, Morffy N, Li Q, Faure L, Chang SH, Yao J, Zheng J, Cai ML, Stanga JP, Flematti GR, et al. 2020. Structure-Function Analysis of SMAX1 Reveals Domains that Mediate its Karrikin-Induced Proteolysis and Interaction with the Receptor KAI2. *The Plant Cell*: tpc.00752.02019.

Liang Y, Ward S, Li P, Bennett T, Leyser O. 2016. SMAX1-LIKE7 Signals from the Nucleus to Regulate Shoot Development in Arabidopsis via Partially EAR Motif-Independent Mechanisms. *The Plant Cell* **28**(7): 1581-1601.

Marzec M, Brewer P. 2019. Binding or Hydrolysis? How Does the Strigolactone Receptor Work? *Trends in Plant Science* **24**(7): 571-574.

Mizuno Y, Komatsu A, Shimazaki S, Xie X, Ishizaki K, Naramoto S, Kyozuka J. 2020. Major components in the KARRIKIN INSENSITIVE2-ligand signaling pathway are conserved in the liverwort, Marchantia polymorpha. *bioRxiv*: 2020.2011.2017.387852.

Nelson DC, Flematti GR, Ghisalberti EL, Dixon KW, Smith SM. 2012. Regulation of Seed Germination and Seedling Growth by Chemical Signals from Burning Vegetation. *Annual Review of Plant Biology* **63**(1): 107-130.

Nelson DC, Flematti GR, Riseborough J-A, Ghisalberti EL, Dixon KW, Smith SM. 2010. Karrikins enhance light responses during germination and seedling development in Arabidopsis thaliana. *Proceedings of the National Academy of Sciences* **107**(15): 7095-7100.

Nelson DC, Scaffidi A, Dun EA, Waters MT, Flematti GR, Dixon KW, Beveridge CA, Ghisalberti EL, Smith SM. 2011. F-box protein MAX2 has dual roles in karrikin and strigolactone signaling in Arabidopsis thaliana. *Proceedings of the National Academy of Sciences* **108**(21): 8897-8902.

Scaffidi A, Waters MT, Bond CS, Dixon KW, Smith SM, Ghisalberti EL, Flematti GR. 2012. Exploring the molecular mechanism of karrikins and strigolactones. *Bioorganic & Medicinal Chemistry Letters* **22**(11): 3743-3746.

Scaffidi A, Waters MT, Ghisalberti EL, Dixon KW, Flematti GR, Smith SM. 2013. Carlactone-independent seedling morphogenesis in Arabidopsis. *The Plant Journal* **76**(1): 1-9.

Scaffidi A, Waters MT, Sun YK, Skelton BW, Dixon KW, Ghisalberti EL, Flematti GR, Smith SM. 2014. Strigolactone Hormones and Their Stereoisomers Signal through Two Related Receptor Proteins to Induce Different Physiological Responses in Arabidopsis. *Plant Physiology* **165**(3): 1221-1232.

Seto Y, Yasui R, Kameoka H, Tamiru M, Cao M, Terauchi R, Sakurada A, Hirano R, Kisugi T, Hanada A, et al. 2019. Strigolactone perception and deactivation by a hydrolase receptor DWARF14. *Nature Communications* **10**(1): 191.

Shabek N, Ticchiarelli F, Mao H, Hinds TR, Leyser O, Zheng N. 2018. Structural plasticity of D3–D14 ubiquitin ligase in strigolactone signalling. *Nature* **563**(7733): 652-656.

Soundappan I, Bennett T, Morffy N, Liang Y, Stanga JP, Abbas A, Leyser O, Nelson DC. 2015. SMAX1-LIKE/D53 Family Members Enable Distinct MAX2-Dependent Responses to Strigolactones and Karrikins in Arabidopsis. *The Plant Cell* **27**(11): 3143-3159.

Stanga JP, Morffy N, Nelson DC. 2016. Functional redundancy in the control of seedling growth by the karrikin signaling pathway. *Planta* **243**(6): 1397-1406.

Stanga JP, Smith SM, Briggs WR, Nelson DC. 2013. SUPPRESSOR OF MORE AXILLARY GROWTH2 1 Controls Seed Germination and Seedling Development in Arabidopsis. *Plant Physiology* **163**(1): 318-330.

Sun YK, Yao J, Scaffidi A, Melville KT, Davies SF, Bond CS, Smith SM, Flematti GR, Waters MT. 2020. Divergent receptor proteins confer responses to different karrikins in two ephemeral weeds. *Nature Communications* **11**(1): 1264.

Swarbreck SM, Guerringue Y, Matthus E, Jamieson FJC, Davies JM. 2019. Impairment in karrikin but not strigolactone sensing enhances root skewing in Arabidopsis thaliana. *The Plant Journal* **98**(4): 607-621.

Taulera Q, Lauressergues D, Martin K, Cadoret M, Servajean V, Boyer F-D, Rochange S. 2020. Initiation of arbuscular mycorrhizal symbiosis involves a novel pathway independent from hyphal branching. *Mycorrhiza*: 1-11.

Toh S, Holbrook-Smith D, Stokes Michael E, Tsuchiya Y, McCourt P. 2014. Detection of Parasitic Plant Suicide Germination Compounds Using a High-Throughput Arabidopsis HTL/KAI2 Strigolactone Perception System. *Chemistry & Biology* **21**(8): 988-998.

Tsuchiya Y, Yoshimura M, Sato Y, Kuwata K, Toh S, Holbrook-Smith D, Zhang H, McCourt P, Itami K, Kinoshita T, et al. 2015. Probing strigolactone receptors in Striga hermonthica with fluorescence. *Science* **349**(6250): 864-868.

Uraguchi D, Kuwata K, Hijikata Y, Yamaguchi R, Imaizumi H, Am S, Rakers C, Mori N, Akiyama K, Irle S, et al. 2018. A femtomolar-range suicide germination stimulant for the parasitic plant Striga hermonthica. *Science* **362**(6420): 1301-1305.

Végh A, Incze N, Fábián A, Huo H, Bradford KJ, Balázs E, Soós V. 2017. Comprehensive Analysis of DWARF14-LIKE2 (DLK2) Reveals Its Functional Divergence from Strigolactone-Related Paralogs. *Frontiers in Plant Science* **8**: 1641.

Villaécija-Aguilar JA, Hamon-Josse M, Carbonnel S, Kretschmar A, Schmidt C, Dawid C, Bennett T, Gutjahr C. 2019. SMAX1/SMXL2 regulate root and root hair development downstream of KAI2-mediated signalling in Arabidopsis. *PLOS Genetics* **15**(8): e1008327.

Walker CH, Siu-Ting K, Taylor A, O'Connell MJ, Bennett T. 2019. Strigolactone synthesis is ancestral in land plants, but canonical strigolactone signalling is a flowering plant innovation. *BMC Biology* **17**(1): 70.

Wang L, Wang B, Jiang L, Liu X, Li X, Lu Z, Meng X, Wang Y, Smith SM, Li J. 2015. Strigolactone Signaling in Arabidopsis Regulates Shoot Development by Targeting D53-Like SMXL Repressor Proteins for Ubiquitination and Degradation. *The Plant Cell* **27**(11): 3128-3142.

Wang L, Xu Q, Yu H, Ma H, Li X, Yang J, Chu J, Xie Q, Wang Y, Smith SM, et al. 2020. Strigolactone and Karrikin Signaling Pathways Elicit Ubiquitination and Proteolysis of SMXL2 to Regulate Hypocotyl Elongation in Arabidopsis thaliana. *The Plant Cell*: tpc.00140.02020.

Waters MT, Gutjahr C, Bennett T, Nelson DC. 2017. Strigolactone Signaling and Evolution. *Annual Review of Plant Biology* **68**(1): 1-31.

Waters MT, Nelson DC, Scaffidi A, Flematti GR, Sun YK, Dixon KW, Smith SM. 2012. Specialisation within the DWARF14 protein family confers distinct responses to karrikins and strigolactones in Arabidopsis. *Development* **139**(7): 1285-1295.

Waters MT, Scaffidi A, Flematti G, Smith Steven M. 2015a. Substrate-Induced Degradation of the α/β-Fold Hydrolase KARRIKIN INSENSITIVE2 Requires a Functional Catalytic Triad but Is Independent of MAX2. *Molecular Plant* **8**(5): 814-817.

Waters MT, Scaffidi A, Moulin SLY, Sun YK, Flematti GR, Smith SM. 2015b. A Selaginella moellendorffii Ortholog of KARRIKIN INSENSITIVE2 Functions in Arabidopsis Development but Cannot Mediate Responses to Karrikins or Strigolactones. *The Plant Cell* **27**(7): 1925-1944.

Yao J, Mashiguchi K, Scaffidi A, Akatsu T, Melville KT, Morita R, Morimoto Y, Smith SM, Seto Y, Flematti GR, et al. 2018. An allelic series at the KARRIKIN INSENSITIVE 2 locus of Arabidopsis thaliana decouples ligand hydrolysis and receptor degradation from downstream signalling. *The Plant Journal* **96**(1): 75-89.

Yao J, Waters MT. 2019. Perception of karrikins by plants: a continuing enigma. *Journal of Experimental Botany*.

Yao R, Ming Z, Yan L, Li S, Wang F, Ma S, Yu C, Yang M, Chen L, Chen L, et al. 2016. DWARF14 is a non-canonical hormone receptor for strigolactone. *Nature* **536**(7617): 469.

Yoneyama K, Xie X, Yoneyama K, Kisugi T, Nomura T, Nakatani Y, Akiyama K, McErlean CSP. 2018. Which are Major Players, Canonical or Non-Canonical Strigolactones? *Journal of Experimental Botany* **111**.

Zhao L-H, Zhou XE, Yi W, Wu Z, Liu Y, Kang Y, Hou L, Waal PWd, Li S, Jiang Y, et al. 2015. Destabilization of strigolactone receptor DWARF14 by binding of ligand and E3-ligase signaling effector DWARF3. *Cell Research* **25**(11): 1219.

Zheng J, Hong K, Zeng L, Wang L, Kang S, Qu M, Dai J, Zou L, Zhu L, Tang Z, et al. 2020. Karrikin Signaling Acts Parallel to and Additively with Strigolactone Signaling to Regulate Rice Mesocotyl Elongation in Darkness. *The Plant Cell*: tpc.00123.02020.

Zhou F, Lin Q, Zhu L, Ren Y, Zhou K, Shabek N, Wu F, Mao H, Dong W, Gan L, et al. 2013. D14–SCFD3-dependent degradation of D53 regulates strigolactone signalling. *Nature* **504**(7480): 406.

FIGURE LEGENDS

Figure 1. Responses of *Arabidopsis thaliana* to desmethyl butenolides are mediated exclusively by KAI2

A, B: Hypocotyl elongation responses to GR24 and CN-debranone enantiomers and their desmethyl equivalents. Data are means ± SE of n = 3 experimental replicates, each consisting of >20 seedlings per sample. Asterisks indicate a significant difference compared to mock-treated seedlings of the same genotype: *, $P < 0.05$; **, $P < 0.01$; ***, $P < 0.001$; ****, $P < 0.0001$ (two-way ANOVA with correction for multiple pairwise comparisons).

C, D: KAI2 protein degradation response to methyl-substituted and desmethyl butenolides. WT Ler seedlings were treated either for 8 h (C) or 2 h (D) with varying concentrations of indicated butenolide compounds.

E: KAI2 and D14 protein degradation response after treatment for 2 h with 1 µM butenolides as indicated. Italicised values below blots indicate mean (± SD) protein levels from n = 3 experimental replicates, expressed relative to the mock-treated control.

F: Yeast two-hybrid assays for KAI2 interaction with SMAX1 (upper panels) or D14 interaction with SMXL7 (lower panels). KAI2 and D14 were fused to GAL4-BD; SMAX1 and SMXL7 were fused to GAL4-AD. Serial 10-fold dilutions of yeast cultures were spotted onto selective growth media supplemented with *rac*-GR24, *rac*-dGR24, or 0.02% acetone control. Images show growth after 3 d at 30 °C. L, Leu; T, Trp; H, His; A, Ade. To improve stringency, interaction assays between KAI2 and SMAX1 lacked Ade, whereas assays between D14 and SMXL7 included Ade.

Figure 2. Rapid and transient induction of *DLK2* transcripts by desmethyl butenolides acting via KAI2

A, D: Levels of *DLK2* transcripts in seedlings of differing genotypes after 2 h of treatment with 1 µM of the indicated butenolide. Asterisks represent significance levels of indicated pairwise comparisons: *, $P < 0.05$; **, $P < 0.01$; ***, $P < 0.001$; ****, $P < 0.0001$; ns, not significant (P

> 0.05). Each genotype was analysed separately by one-way ANOVA with correction for multiple pairwise comparisons.

B, E: Levels of *DLK2* transcripts in seedlings after 2 h of treatment with varying concentrations of the indicated butenolide.

C, F: Levels of *DLK2* transcripts in seedlings after treatment with 1 µM of the indicated butenolide for varying periods of time. Seedling genotypes are L*er* (B, C) and *Atd14-1* (E, F). For all panels, data are means ± SE of n = 3 biological replicates.

Figure 3. Arabidopsis KAI2 but not AtD14 shows enhanced responses to desmethyl butenolides

A, B: Thermal shift response assays of SUMO-tagged AtKAI2 (A) or AtD14 (B) in response to 0–200 µM methyl-substituted butenolides (left panels) or desmethyl butenolides (right panels). Data are means of four technical replicates.

C, D: Intrinsic tryptophan fluorescence measurements of SUMO-tagged AtKAI2 (C) and AtD14 (D) in response to varying concentrations of each ligand. Dissociation constants (Kd) were estimated by non-linear regression where feasible; numbers in parentheses indicate 95% CI. n.d., not determinable. Data are means ± SE of four technical replicates.

Figure 4. Effects of the butenolide methyl substituent on KAI2 and D14 hydrolase activity

A, B: Monitoring of GR24 and dGR24 hydrolysis by AtKAI2 (A) and AtD14 (B) using HPLC. Reactions contained 2 mg/mL SUMO-AtKAI2, SUMO-AtD14, or an equivalent volume of buffer, and 500 µM of a single enantiomer of GR24 or dGR24 as indicated. Reactions were sampled approximately 1.5 min after addition of protein to ligand (0 h) and then re-sampled every 2 h thereafter. Because the activity of SUMO-AtD14 towards dGR24^{5DS} was so high, a further set of reactions containing a ten-fold dilution of protein (AtD14 1/10) was also performed. Data are expressed as percentage of ligand remaining relative to the buffer-only sample at 0 h. Data are means ± SD of n = 3 replicate reactions run in parallel.

C–F: Hydrolysis competition assays using dYLG as the preferred fluorogenic substrate for AtKAI2 (C, E) or YLG for AtD14 (D, F). Reactions contained 5 µM dYLG or YLG, 1 µg of SUMO

fusion protein, and varying concentrations of competitor butenolides as indicated. Hydrolysis was measured by the change in fluorescence over 15 minutes. Data are expressed relative to the hydrolysis observed in the absence of competitor. Data are means ± SE of n = 3 technical replicates. IC50 values were estimated by non-linear regression; values in parentheses indicate asymmetric 95% CI; n.d., not determinable.

Figure 5. Enhanced responses to desmethyl butenolides are evolutionarily ancient

A: Thermal shift response of SUMO-SmKAI2a fusion protein to increasing concentrations of GR24ent-5DS and dGR24ent-5DS. Data are means of four technical replicates.

B: Inhibition of intrinsic tryptophan fluorescence of SUMO-SmKAI2a by GR24$^{ent\text{-}5DS}$ and dGR24$^{ent\text{-}5DS}$ ligands. Data are means ± SE of 4 technical replicates.

C: Seedling hypocotyl elongation responses to dGR24^{5DS} and dGR24$^{ent\text{-}5DS}$. Two homozygous transgenic lines expressing *SmKAI2a* from the *AtKAI2* promoter, which incompletely complement the *kai2-2* phenotype (Waters et al. 2015), are shown. Data are means ± SE of n = 20 seedlings; each dot corresponds to an individual. Asterisks indicate a significant difference compared to mock-treated seedlings of the same genotype: *, $P < 0.05$; ***, $P < 0.001$; ****, $P < 0.0001$ (two-way ANOVA with correction for multiple pairwise comparisons).

D: *DLK2* transcript levels in *KAI2:SmKAI2a* transgenics treated with 10 µM dGR24$^{ent\text{-}5DS}$ for 2 h h. Transcripts were normalised to *CACS* reference transcripts; data are means ± SE of n = 3 biological replicates. Inset shows the same data but on a smaller scale; ***, $P < 0.001$; ****, $P < 0.0001$ (two-way ANOVA with correction for multiple pairwise comparisons).

E: *DLP1* transcript levels in wild type and *max2* mutant gametophytes of *Marchantia polymorpha* treated with 1 µM butenolides for 6 h. Transcripts were normalised to *Actin* reference transcripts; data are means ± SE of n = 3 biological replicates. Inset shows the same data for *Mpmax2-1* but on a smaller scale. Groups labelled with different lowercase letters are significantly different at $\alpha = 0.05$; each genotype was analysed separately by one-way ANOVA with correction for multiple pairwise comparisons.

SUPPORTING INFORMATION

Additional supporting information may be found in the online version of this article:

Figure S1. Synthesis, separation and stereochemical assignment of enantiomers of desmethyl-GR24 and desmethyl-CN-debranone

Figure S2. Intrinsic tryptophan fluorescence assays are incompatible with karrikin ligands

Figure S3. Response of rice KAI2 & D14 proteins to methyl-substituted and desmethyl butenolides

Figure S4. Thermal shift responses of Arabidopsis and rice KAI2 proteins to non-bioactive butenolides

Figure S5. Two KAI2 homologues from *Glycine max* respond preferentially to desmethyl-GR24

Figure S6. Thermal shift responses of Arabidopsis and rice D14 proteins to non-bioactive butenolide enantiomers

Figure S7. Atkai2 S95A binds dGR24$^{ent\text{-}5DS}$ but cannot mediate responses *in planta*

Figure S8. *MpDLP1* transcripts are mis-regulated in *Mpmax2-1*

Table S1. Oligonucleotides used in this study

Methods S1. Chemical synthesis

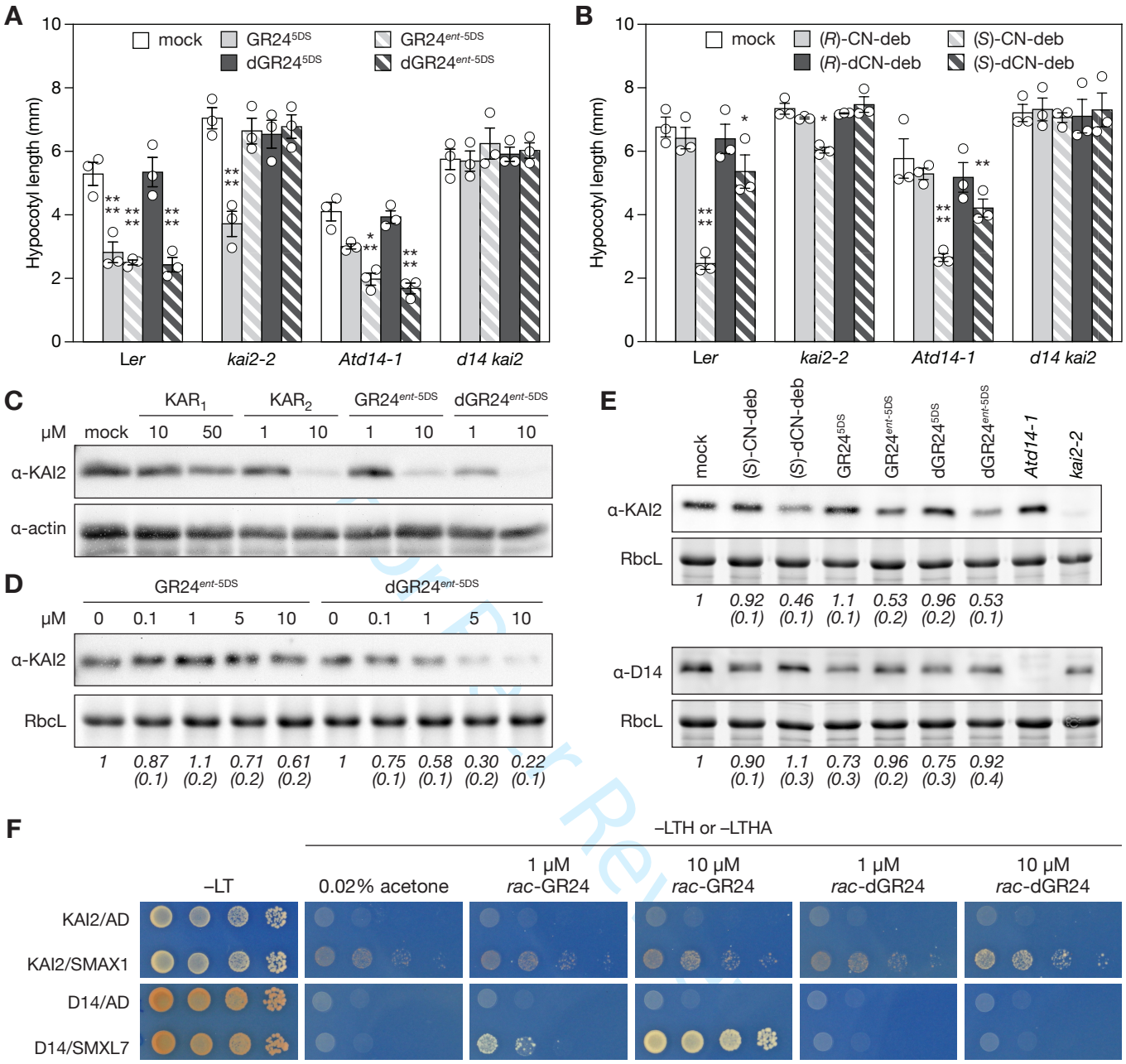
A
mock
GR24 5DS
dGR24 5DS
GR24 ent-5DS
dGR24 ent-5DS
Hypocotyl length (mm)
Ler
kai2-2
Atd14-1
d14 kai2
B
mock
(R)-CN-deb
(S)-CN-deb
(R)-dCN-deb
(S)-dCN-deb
Hypocotyl length (mm)
Ler
kai2-2
Atd14-1
d14 kai2
C
KAR1
KAR2
GR24 ent-5DS
dGR24 ent-5DS
μM mock 10 50 1 10 1 10 1 10
α-KAI2
α-actin
D
GR24 ent-5DS
dGR24 ent-5DS
μM 0 0.1 1 5 10 0 0.1 1 5 10
α-KAI2
RbcL
1 0.87 (0.1) 1.1 (0.2) 0.71 (0.2) 0.61 (0.2) 1 0.75 (0.1) 0.58 (0.1) 0.30 (0.2) 0.22 (0.1)
E
mock
(S)-CN-deb
(S)-dCN-deb
GR24 5DS
GR24 ent-5DS
dGR24 5DS
dGR24 ent-5DS
Atd14-1
kai2-2
α-KAI2
RbcL
1 0.92 (0.1) 0.46 (0.1) 1.1 (0.1) 0.53 (0.2) 0.96 (0.2) 0.53 (0.1)
α-D14
RbcL
1 0.90 (0.1) 1.1 (0.3) 0.73 (0.3) 0.96 (0.2) 0.75 (0.3) 0.92 (0.4)
F
–LTH or –LTHA
–LT
0.02% acetone
1 μM rac-GR24
10 μM rac-GR24
1 μM rac-dGR24
10 μM rac-dGR24
KAI2/AD
KAI2/SMAX1
D14/AD
D14/SMXL7